Article

Performance Assessment of Wood Ash and Bone Char for Manganese Treatment in Acid Mine Drainage

Ivana Smičiklas [1,*], **Bojan Janković** [1], **Mihajlo Jović** [1], **Jelena Maletaškić** [1], **Nebojša Manić** [2] and **Snežana Dragović** [1]

1 "VINČA" Institute of Nuclear Sciences—National Institute of the Republic of Serbia, University of Belgrade, Mike Petrovića Alasa 12-14, P.O. Box 522, 11001 Belgrade, Serbia; bojan.jankovic@vin.bg.ac.rs (B.J.); mjovic@vin.bg.ac.rs (M.J.); jelena.pantic@vin.bg.ac.rs (J.M.); sdragovic@vin.bg.ac.rs (S.D.)
2 Faculty of Mechanical Engineering, University of Belgrade, Kraljice Marije 16, P.O. Box 35, 11120 Belgrade, Serbia; nmanic@mas.bg.ac.rs
* Correspondence: ivanat@vin.bg.ac.rs

Abstract: Developing efficient methods for Mn separation is the most challenging in exploring innovative and sustainable acid mine drainage (AMD) treatments. The availability and capacity of certain waste materials for Mn removal warrant further exploration of their performance regarding the effect of process factors. This study addressed the influence of AMD chemistry (initial pH and concentrations of Mn, sulfate, and Fe), the solid/solution ratio, and the contact time on Mn separation by wood ash (WA) and bone char (BC). At an equivalent dose, WA displayed higher neutralization and Mn removal capacity over the initial pH range of 2.5–6.0 due to lime, dicalcium silicate, and fairchildite dissolution. On the other hand, at optimal doses, Mn separation by BC was faster, it was less affected by coexisting sulfate and Fe(II) species, and the carbonated hydroxyapatite structure of BC remained preserved. Efficient removal of Mn was feasible only at final pH values ≥ 9.0 in all systems with WA and at pH 6.0–6.4 using BC. These conclusions were confirmed by treating actual AMD with variable doses of both materials. The water-leaching potential of toxic elements from the AMD/BC treatment residue complied with the limits for inert waste. In contrast, the residue of AMD/WA treatment leached non-toxic quantities of Cr and substantial amounts of Al due to high residual alkalinity. To minimize the amount of secondary waste generated by BC application, its use emerges particularly beneficial after AMD neutralization in the finishing step intended for Mn removal.

Keywords: acid mine drainage; Mn separation; waste valorization; wood ash; bone char

1. Introduction

Acid drainage resulting from mining activities poses a substantial worldwide problem for protecting and managing water resources, sediments, and soil [1–3]. The adjustment of pH and elimination of metal ions, such as manganese (Mn), iron (Fe), copper (Cu), zinc (Zn), arsenic (As), cadmium (Cd), and lead (Pb), are fundamental objectives of acid mine drainage (AMD) remediation processes (physical, chemical, and biological), which implementation depends on reckoning environmental, technical, and economic factors [4]. The neutralization of AMD by conventional chemicals (lime, pebble quicklime, caustic soda, soda ash briquettes, ammonia, magnesium hydroxide, and magna lime) is by far the most utilized [5]. Nevertheless, the neutralization is often combined with other technologies (aeration, flocculation, coagulation, filtration, etc.) to meet effluent quality requirements [6].

The actual cost of the AMD treatment approach includes the price of the chemical reagent and the cost of energy needed to transport the materials [7], thus, the efficiency of alternative low-cost and locally available materials has been progressively studied in recent years to ensure the sustainability of AMD treatment. A special impetus to the research of

waste materials applicability in AMD remediation is given through the European Union's ambition to reduce its consumption footprint and double its circular material use rate in the coming decade [8]. Alkaline industrial wastes and byproducts, for instance, the bauxite residue, coal fly ash, byproducts of industrial smelting of metals (slags), and quicklime manufacturing, are being proposed for AMD remediation [9,10]. Likewise, abundant organic waste materials, such as rice husks and dairy manure compost, exhibit high metal removal efficiency, while chitin and chitosan additionally act as neutralizing and sulfate removal agents [11].

Compared to other toxic metals in AMD, manganese (Mn) treatment is the most difficult due to its complex chemistry and high pH values necessary for precipitation. Given various Mn oxidation states, the precipitation occurs at a pH of 9.0–9.5, but in some cases, even a pH of 10.5 is necessary for complete removal [5]. Concentrations of Mn in surface waters are frequently less than 200 µg/L and rarely exceed 1 mg/L [12], whereas, in mining water, they can be orders of magnitude higher, reaching several hundred mg per liter in highly contaminated mine drainage [13]. These effluents' impacts on natural freshwaters encompass the temporal changes in dissolved Mn concentrations, Mn behavior in the suspended load and bottom sediments, and the geochemical fate of other trace elements with a high affinity for Mn-oxyhydroxides [13,14]. The two fundamental mechanisms in control for Mn removal from AMD are precipitation and sorption, both of which are dependent upon Eh-pH conditions, the concentration of Mn, and competing ions. The weaknesses of Mn chemical treatment include the high costs of pH increase and the high pH of the sludge, thus, effective removal of Mn continues to be a challenge.

Various affordable and waste-derived materials have been investigated so far for Mn separation [15,16]; however, their applicability in actual AMD is more challenging due to the strong acidity and competitive species [15]. The usability of materials generated by wood combustion (wood ash) and thermal treatment of animal bones (bone char) for treating Mn in AMD was seldom explored, yet with encouraging results. The intensive use of wood as an energy-supply source in some regions urged a search for methods of wood ash utilization to minimize the environmental risks caused by disposal. Its chemical composition fluctuates among species of timber, combustion temperature, type, and hydrodynamics of the furnace [17]. Nevertheless, the major components, i.e., lime (CaO), portlandite ($Ca(OH)_2$), and calcite ($CaCO_3$), make it broadly applicable in pH control of AMD. A comparison of $Ca(OH)_2$ and wood ash in AMD treatment (initial Mn concentration 6.2 mg/L), revealed that dosing of both materials increased the solution pH from 3.5 to 8.3, causing a more effective drop in Mn concentration by wood ash (2.68 mg/L) than by $Ca(OH)_2$ (4.35 mg/L) [18]. Wood ash was found to act by precipitation, co-precipitation, and adsorption of trace metals from AMD, including Fe, As, Co, Cu, Ni, Zn, Mg, Al, and Mo. Moreover, the sludge from wood ash application had better settling capacities than the $Ca(OH)_2$ generated sludge.

The bone char obtained by treating ground animal bones at moderate temperatures is composed of calcium phosphate (57–80%), calcium carbonate (6–10%), and carbon (7–10%) [19]. The bone mineral component is commonly referred to as carbonated hydroxyapatite [20]. Manganese removal study from AMD by a commercial bone char suggested the intraparticle diffusion as the main rate-limiting step with contribution from boundary layer diffusion when smaller sizes of bone char particles are used [21]. The bone char not only removed metal species from the effluent but also increased its pH value. At the equal solid/liquid ratio, equilibrium sorbed amounts of Mn were higher at initial pH 6.5 (maximum sorption capacity, q_m = 22 mg/g) than at initial pH 5.0 (q_m = 14 mg/g). In continuous fixed bed column runs, no significant change in the breakthrough volume was detected with different flow rates, but the breakthrough volume increased by increasing the initial pH from 2.9 to 5.5 [22]. The maximum loading capacity of bone char in continuous tests with AMD effluents was 6.03 mg/g. The outcomes of studies using synthetic hydroxyapatite [23], bioapatite obtained from fish bone (Apatite II^{TM}) [24], and natural fluorapatite [25], also indicate the potential for efficient Mn removal at pH values considerably

lower than those required for Mn-hydroxide precipitation. Moreover, apatite materials are suitable for the separation of not only Mn but diverse pollutants that may occur in AMD, controlling trace element mobility to surrounding soils and surface water [26–28].

While the integration of wood ash and thermally treated animal bones in Mn treatment aligns with circular economy principles and holds promise, a significant gap in understanding their efficacy still exists due to inadequate recognition of the impact of AMD chemistry and other process variables on their performance. Notably, the levels of coexisting Fe ions and the relevance of the Fe to Mn ratio are important issues requiring more extensive investigation [13]. Thus, the main objective of this study was to address these knowledge gaps and provide deeper insights into the performance of wood ash and bone char in Mn separation.

The influence of process variables, specifically reagent dose, reaction time, initial pH, Mn concentration, and the concentrations of sulfate and coexisting Fe ions, on the efficiency of Mn removal by wood ash and bone char was addressed. Owing to distinct physicochemical properties, neutralization capacities, and mechanisms for Mn removal, these materials are anticipated to manifest divergent responses to variations in process factors. The impacts of factors were ascertained through two approaches: (i) a classical methodology involving the alteration of one independent factor across multiple levels while keeping others constant, and (ii) an experimental design approach encompassing the simultaneous variation of all factors to evaluate the intensity of their effects and glean insights into potential interactions. Furthermore, the study assessed the practical viability of wood ash and bone char in treating actual AMD sourced from the lead and zinc mine "Sase" in Srebrenica, Bosnia and Herzegovina. Additionally, an examination was conducted regarding the leaching potential of hazardous elements from the resultant residues and prospects of Mn recovery.

2. Materials and Method

2.1. Wood Ash and Bone Char Preparation and Characterization

The wood ash used in the study (WA) represents the bottom ash from the combustion process in the conventional 250 kW boiler fueled by wood chips. During the combustion of the wood chips, mainly pine wood, the average temperature in the combustion chamber was 800 °C. The WA sample containing bigger particles (0.1–10 mm) was collected from the ash pane at the bottom of the boiler, crushed in a ball mill, and sieved through a 1 mm screen to make representative material for further testing and analysis.

The bone char (BC) was prepared by treating crushed bovine bones in an electrical furnace (ELEKTRON, Banja Koviljača, Serbia) at 400 °C in ambient air for 4 h, according to the procedure previously described [29]. The sample mass loss of approximately 33% is associated with the loss of water and decomposition of the organic phase, which was found advantageous for obtaining a high-capacity sorbent for trace metals [29,30]. The sample was homogenized and ground to a particle size < 0.2 mm.

The pH values and electrical conductivity (EC) of WA and BC were determined in deionized water at a solid/liquid ratio of 1:5, using the inoLab pH Level 1 and inoLab Cond 7110 (WTW, Weilheim, Germany), respectively. The point of zero charge (pH_{PZC}) was determined in an inert electrolyte by adjusting its initial pH values and monitoring the equilibrium pH values [31]. The investigated materials (0.1 g) were agitated in an overhead shaker (10 rpm) with 20 mL of 0.1 mol/L and 0.01 mol/L KNO_3 solutions with the initial pH in the range 1–12 (adjusted using 0.1 M HNO_3 and 0.1 M KOH). The suspensions were centrifugated and filtrated, and the final pH values were measured in clear supernatants. The pH shift upon reaction with the BC and WA ($\Delta pH = pH_{final} - pH_{initial}$) was calculated, and the pHpzc was identified at $\Delta pH = 0$.

Pseudo-total element concentrations were measured by Inductively Coupled Plasma Optical Emission Spectrometry (ICP-OES) on the Avio 200 instrument (Perkin Elmer, Shelton, CT, USA). The samples were prepared by precise mass measurement and digestion

with heating in a mixture of HNO_3 and HCl (3:1) for 4 h under reflux. The results of two replicated analyses are reported in % or mg/kg dry material.

Identification of crystalline phases was made at room temperature by X-ray powder diffraction (XRPD) using Ultima IV (Rigaku, Tokyo, Japan) diffractometer equipped with Cu Kα1,2 radiation using a generator voltage (40.0 kV) and a generator current (40.0 mA). The range of 5–70°2θ was used for all powders in a continuous scan mode with a scanning step size of 0.02° and at a scan rate of 5°/min. Phase analysis was performed by the PDXL2 software (version 2.0.3.0, Rigaku, Tokyo, Japan) [32], with reference to the patterns of the International Centre for Diffraction Data database (ICDD) version 2012 [33]. All the structure information was taken from the American Mineralogist Crystal Data Structure Base (AMCDSB) [34].

2.2. Effects of Independent Process Factors on Mn Removal by BC and WA

Manganese removal experiments were performed in the batch mode by mixing the reagents and solutions in 50 mL polypropylene tubes on the Heidolph Reax overhead shaker (10 rpm), centrifugation for 5 min at 9000 rpm, and filtering through syringe filters with a 0.45 μm pore size. Synthetic AMD solutions were prepared from p.a. purity salts ($MnCl_2 \times 4\,H_2O$, Na_2SO_4, and $FeCl_2 \times 4\,H_2O$, Merck KGaA, Darmstadt, Germany).

The initial pH effect on Mn removal was studied at a fixed dose of BC and WA (1 g/L), Mn concentration (100 mg/L), and contact time (24 h) while adjusting the pH in the range of 1.5–6.0 by adding dropwise 0.1 mol/L HCl or 0.01 mol/L NaOH.

The effect of BC and WA dose variation (0.3–10 g/L) was examined for three initial concentrations of Mn (5 mg/L, 50 mg/L, and 100 mg/L) at the fixed initial pH of 2.5 and a contact time of 24 h.

Based on the above-described experiments, the doses for treating 100 mg/L Mn solution at initial pH 2.5 were fixed for investigated waste materials (1.2 g/L WA and 10 g/L BC), and the influence of contact time (5 min–24 h), sulfate concentration (500–10,000 mg/L), and Fe concentrations (5–500 mg/L) were investigated.

The experiments were conducted in duplicate. Manganese and Fe concentrations were measured using the ICP-OES technique, and the efficiency of each treatment was calculated.

2.3. Assessment of the Effects of Process Variables and Their Interactions—Experimental Design

Previous experiments showed that all investigated factors affect the efficiency of Mn removal from synthetic AMD at the constant levels of other independent process variables. To better understand the system response under the influence of several experimental factors, the experimental design (DOE) approach was applied. Table 1 denotes selected independent factors and their lower and higher values.

Table 1. Selected independent factors and their levels.

Level	Factor						
	A	**B**	**C**	**D**	**E**	**F**	**G**
	Reagent Type	Mn Conc. (mg/L)	Sulfate Conc. (mg/L)	Fe Conc. (mg/L)	Time (h)	Initial pH	Reagent Dose (g/L)
−1	BC	5	100	5	0.5	2.0	0.5
+1	WA	100	10,000	400	24	4.5	5.0

The fractional factorial design matrix in 16 runs was chosen as a screening technique. In the two-level DOE, one treatment setup refers to a combination of levels of all selected independent factors, and it is helpful to assess their contribution and identify essential interactions between the variables. The fractional factorial design matrix was created, and the results were analyzed using the statistical software (Minitab, demo version, Minitab LLC., State College, PA, USA). As the primary output variable, the efficiency of Mn removal

was determined for each experimental run. Furthermore, final pH values and Fe removal efficiency were monitored.

2.4. AMD Treatment

The actual AMD used in the study was a sample of pit water collected at the lead and zinc mine "Sase" Srebrenica (Bosnia and Herzegovina). Treatments have been conducted at constant contact time (24 h) and mixing speed (10 rpm) by varying the dose of WA (1–3 g/L) and BC (1–30 g/L). The pH values of AMD were determined before and after the treatments, and the ICP-OES was used to determine the concentrations of Mn and other toxic metals.

2.5. Stability of the AMD Treatment Residues

The selected residues obtained after AMD treatments were further investigated regarding the leaching potential and metal recovery. Two replicated experiments were conducted for each residue. Solid phases following the AMD reaction with 2.5 g/L WA and 30 g/L BC were separated by filtration (qualitative filter paper), dried at 100 °C for 24 h, and exposed to leaching by deionized water at a 1:10 solid-to-solution ratio for 20 h, using an overhead laboratory shaker at 20 rpm [35]. After filtering the leachates (0.45 μm pore size syringe filters), the concentration of elements was determined using the ICP-OES. Furthermore, the possible reuse of the materials and recovery of AMD major cations from WA/AMD and BC/AMD residues was investigated using HCl solutions with concentrations of 0.01 mol/L, 0.1 mol/L, and 1 mol/L. The solid-to-solution ratio was maintained at 5 g/L. The suspensions were agitated for 24 h, and the metal concentrations and final pH values were measured in the supernatants after centrifugation and filtration.

3. Results

3.1. Chemical and Mineralogical Characteristics of WA and BC

According to the results in Table 2, the primary metals in WA were Ca (31.0%), K (15.5%), and Mg (5.3%), as reported for a variety of wood and woody biomass ashes [36,37], followed by Al (2.36%), Mn (1.22%), Na (0.844%) and Fe (0.398%).

High Mn concentrations are characteristic for wood ash, i.e., a mean concentration of 13,160 mg/kg (min. 775 mg/kg, max. 35,740 mg/kg) was reported considering the ashes of 28 types of wood and woody biomass [36]. Among the trace metals, copper (163 mg/kg) and Cr (40.6 mg/kg) were dominant, whereas Pb, Cd, and As concentrations in WA were below detection limits. The content of P was 2.06%.

The complex mineralogy of pristine WA is shown in Figure 1a. The shape of the XRD baseline indicates the presence of amorphous solids, while the principal crystalline phases were dicalcium silicate (Sy: Ca_2SiO_4) and fairchildite (F: $K_2Ca(CO_3)_2$). Although calcite is a common component in the bottom biomass ashes [18,38], ash mineralogy is controlled by the relative ratios of the dominant ash-forming cations and reaction temperature. The formation of fairchildite instead of calcite relies on the wood's initial K:Ca ratio [39] and can be associated with a high K content in the WA sample (Table 2). The interaction between Mg and Ca or K is insignificant during ash formation, usually leading to the periclase (P: MgO) formation [39], as identified in the WA. The relatively high level of CaO (L) in WA is typical for wood sources. Furthermore, the minor shares of potassium dithionate (Ks: $K_2S_2O_6$), anorthite (An: $CaAl_2Si_2O_8$), and potassium-iron-phosphate phase (Kp: $KFePO_4$) were present in the sample.

P: MgO   C: $CaCO_3$
L: CaO   Ns: $Na_4Ca_4Si_6O_{18}$
F: $K_2Ca(CO_3)_2$ Kl: $KAlO_2$
Sy: Ca_2SiO_4 Fp: $(FeMn)_3PO_4$
An: $CaAl_2Si_2O_8$ Kc: $K_2Ca_6Si_4O_{15}$
Kp: $KFePO_4$ KaS: $KAl(SO_4)_2(H_2O)_{12}$
Ks: $K_2S_2O_6$ Ks1: $K_2Si_4O_9$

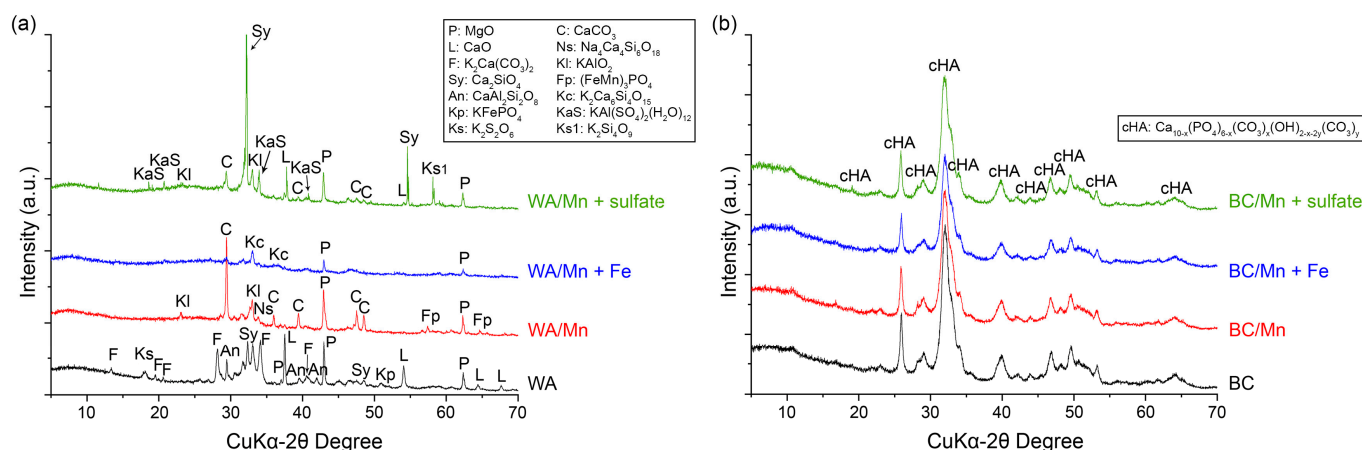cHA: $Ca_{10-x}(PO_4)_{6-x}(CO_3)_x(OH)_{2-x-2y}(CO_3)_y$

Figure 1. XRD patterns of pristine samples (**a**) WA and (**b**) BC, and the solid residues of their interaction with solutions having 100 mg/L Mn (red line); 100 mg/L Mn and 500 mg/L Fe (blue line), 100 mg/L Mn + 10,000 mg/L SO_4 (green line). Initial pH 2.5, dose 1.2 g/L WA and 10 g/L BC, contact time 24 h.

Table 2. pH, pH_{PZC}, electrical conductivity, and pseudo-total concentrations of elements in WA and BC.

Parameter	WA		BC	
pH	12.6 ± 0.1		7.7 ± 0.1	
EC (mS/cm)	34.8 ± 0.5		0.887 ± 0.035	
pH_{PZC}	12.0 ± 0.1		6.9 ± 0.2	
Element	Concentration	Units	Concentration	Units
P	2.06 ± 0.08	%	18.6 ± 0.6	%
Ca	31.0 ± 2.8	%	37.7 ± 1.7	%
Mg	5.30 ± 0.15	%	0.796 ± 0.032	%
K	15.5 ± 0.4	%	104 ± 5	mg/kg
Na	0.844 ± 0.031	%	0.475 ± 0.018	%
Al	2.36 ± 0.13	%	<LOD	-
Mn	1.22 ± 0.06	%	0.953 ± 0.031	mg/kg
Fe	0.398 ± 0.012	mg/kg	31.6 ± 1.1	mg/kg
Cu	163 ± 6	mg/kg	0.897 ± 0.033	mg/kg
Cr	40.6 ± 0.7	mg/kg	3.51 ± 0.17	mg/kg
Ni	14.8 ± 0.1	mg/kg	<LOD	-
Zn	6.59 ± 1.17	mg/kg	147 ± 8	mg/kg
Co	5.45 ± 0.22	mg/kg	<LOD	-
V	4.27 ± 0.34	mg/kg	<LOD	-
Se	0.295 ± 0.015	mg/kg	<LOD	-
Pb	<LOD	-	0.599 ± 0.030	mg/kg
As	<LOD	-	<LOD	-
Cd	<LOD	-	<LOD	-

LOD (Limit of Detection, mg/L)—Pb: 0.007, As: 0.005, Cd: 0.001, Al: 0.005, Co: 0.003, V: 0.001, Se: 0.002, Ni: 0.002.

The structure of the bone mineral phase was maintained after the treatment, and the XRD spectrum of pristine BC shows only peaks corresponding to carbonated hydroxyapatite (cHA: $Ca_{10-x}(PO_4)_{6-x}(CO_3)_x(OH)_{2-x-2y}(CO_3)_y$) (Figure 1b). The chemical composition of the BC (Table 1) supports high Ca and P content (37.7% and 18.6%). Magnesium (0.796%) and Na (0.475%) are typical bone constituents as well [40]. The potassium and trace elements content in BC was significantly lower than in WA, except for Zn (147 mg/kg).

While BC exhibited a mildly alkaline reaction (pH 7.7), WA acts as a strong base in water, bringing pH to 12.6. Wood bottom ash samples generally exhibit higher pH and better neutralization capacity than wood fly ash [41]. Consequently, the water solubility of WA constituents provoked EC of 34.8 mS/cm, much higher compared to BC (0.887 mS/cm).

The pH$_{PZC}$ of BC was found to be at pH 6.9 (Table 2, Supplementary Material Figure S1), in good agreement with near-neutral values determined for hydroxyapatite samples obtained by different procedures and from different precursors [29,42–44]. In line with the literature data [45], the pH$_{PZC}$ of WA was in the alkaline region (12 ± 0.1).

3.2. The Influence of Initial pH on Mn Removal

Removal of Mn from 100 mg/L solutions varied significantly with the change in the initial pH and the reagent type, maintaining the experiment's other conditions constant (Figure 2a,b).
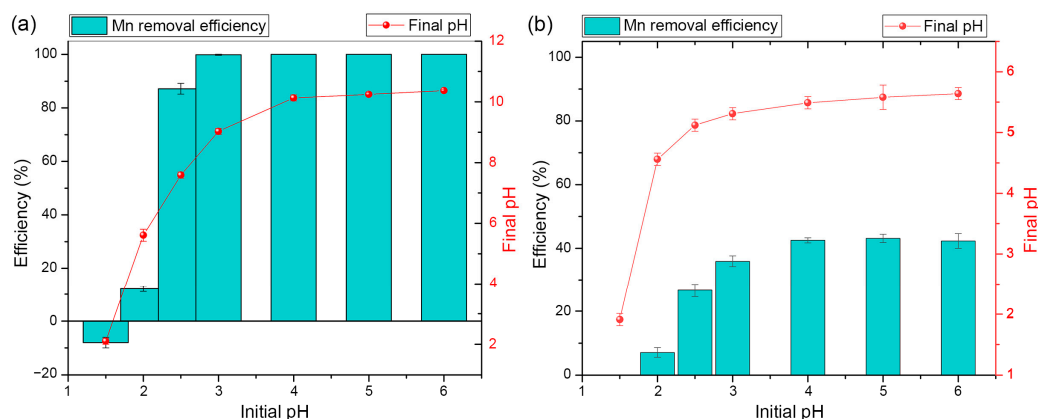
Figure 2. Relations between the initial pH, final pH, and Mn removal efficiency in the system with WA (**a**) and BC (**b**). Dose 1 g/L, Mn concentration 100 mg/L, 24 h contact time.

Manganese concentration after the experiment conducted at an initial pH of 1.5 remained virtually unchanged using BC, whereas the net increase was detected following WA application. At the 1 g/L dose, the WA and BC neutralization capacity was exhausted, marginally raising the pH to 2.1 and 1.9, respectively. Under such pH conditions, the leaching of Mn from the WA composition (Table 2) occurred. The reaction of WA and BC with the solution of initial pH 2.0 resulted in a 12.1% and 7.1% decrease in Mn concentration. WA application triggered a drastic increase in process efficiency (to 87.2%) already at an initial pH of 2.5, and with a further initial pH increase (3–6), Mn was removed completely (99.9–100%). The efficiency of BC improved to 42.5% with increasing initial pH to 4.0 and remained at a constant level up to the initial pH of 6.0.

Excellent WA performance was related to the abrupt increase in the final pH (by 3.6–6.1 pH units, depending on the initial pH), and the Mn was eliminated in all systems with final pH ≥ 9.0 (Figure 2a). Final pH values increased as well after BC addition, reaching a maximum of 5.6 (Figure 2b). The most significant changes in final pH were observed in the initial pH range 2.0–3.0 (by 2.5–2.3 pH units) while retarded with a further increase in initial pH values. As demonstrated for mineral and biogenic samples, the apatite dissolution rate decreases by increasing pH [24,25].

According to the mine drainage pollution classes suggested by Hill [1], Class I is described as acidic with a typical pH range of 2.0–4.5, and Class II denotes partially oxidized or neutralized drainage (pH 3.5–6.6). By applying an equivalent dose of materials, WA showed a higher capacity to separate Mn over the initial pH range corresponding to these categories. The amount of Mn removed per unit mass of reagent varied between 12.1 mg/g and 100 mg/g for WA and between 7.1 mg/g and 42.5 mg/g for BC (Supplementary Material Figure S2a).

3.3. The Influence of Reagent Dose and Mn Concentration

The effect of the solid/solution ratio on the removal efficiency of Mn was examined at a constant initial pH value of 2.5. As displayed in Figure 3a,c, an increase in the dose of reagents affects the decrease in Mn concentration in the solution, but the absolute values of these changes depend on the type of added material and the initial Mn concentration.
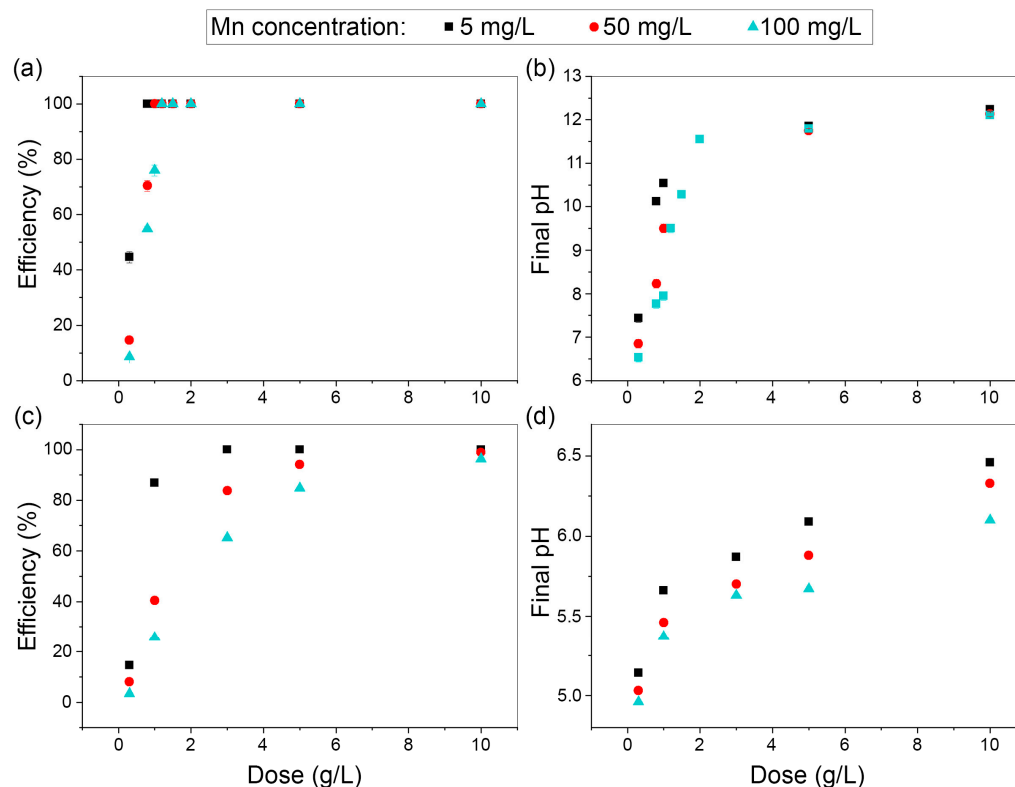

Figure 3. Effect of reagent dose on Mn removal efficiency and final pH values in the systems with WA (**a**,**b**) and BC (**c**,**d**). Initial pH 2.5, contact time 24 h.

Using WA, Mn was removed entirely from the 5 mg/L solution at a dose of 0.8 g/L. For the complete removal of 50 mg/L Mn, the dose of 1 g/L was necessary, while adding 1.2 g/L WA was successful for the treatment of 100 mg/L Mn solution. The amount of Mn removed per unit mass of WA commonly increased with the increase in its initial concentration but varied broadly with the change in the reagent dose (Supplementary Material Figure S2b).

Increasing Mn removal efficiency was also observed with increasing BC dose (Figure 3c), but effective treatment of acidic wastewater required considerably higher BC amounts than WA. Adding 3 g/L BC, Mn was separated from the 5 mg/L solution below the detection limit. Process efficiency continuously increased in solutions with 50 and 100 mg/L Mn with the increase in BC dose, reaching 99.0 and 96.2%, respectively, for 10 g/L BC. The highest Mn removal from 5 mg/L solution per unit mass of BC was 1.6 mg/g at the dose of 3 g/L (Supplementary Material Figure S2c). Starting with more concentrated Mn solutions (50 and 100 mg/L), maximally 20.0 mg/g and 25.5 mg/g BC were respectively removed with the BC dose of 1 g/L. With a dose rise to 10 g/L, the amount of Mn removed per gram of BC declined to 5.0 mg/g and 9.6 mg/g.
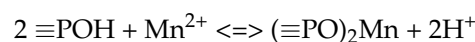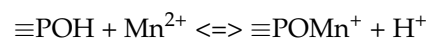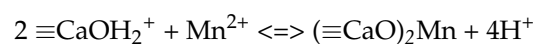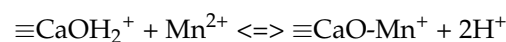
As the Mn concentration in the solution increased, raising the WA dose from 0.8 to 1.2 g/L was necessary to reach a final pH value of ~9 (Figure 3b). Given the pH critical for Mn's complete removal by wood ash, it was associated with hydroxide/oxyhydroxide precipitation [38]. An additional increase in the amount of WA can be considered unnecessary and unfavorable from the treated water quality point of view, i.e., high alkalinity.

Compared to pristine WA, in the representative solid residue of WA/synthetic AMD interaction (initial pH 2.5, 1.2 g/L WA, 100 mg/L Mn), the MgO phase was preserved, whereas diffraction maximums of CaO and Ca_2SiO_4 disappeared, signifying their role in bringing the solution pH to an alkaline region (Figure 1a). In addition to lime, calcium silicate is known for neutralizing the active acidity in AMD [3] by capturing free H^+ ions and forming neutral H_4SiO_4, which remains in the bulk solution. The fairchildite (F: $K_2Ca(CO_3)_2$) was also dissolved, while calcite (C: $CaCO_3$) precipitated. Additional precipitates were identified as tetrasodium tetracalcium cyclo-hexasilicate (Ns: $Na_4Ca_4Si_6O_{18}$), potassium aluminum oxide (Kl: $KAlO_2$), and graftonite (Fp: $(FeMn)_3PO_4$).

Quite the opposite, Mn removal in the presence of BC occurred at final pH values of 5.0–6.5 (Figure 3d), far from the Mn precipitation threshold. The final pH increased with the increase in BC dose at all tested Mn concentrations, similarly as in the work of Sicupira et al. [21], displaying that the BC/AMD ratio is a vital operating variable in Mn removal by bone char.

The mineral composition of BC remained unaffected after the interaction of 10 g/L BC with 100 mg/L Mn solution at initial pH 2.5, but a decrease in the intensity of the carbonated hydroxyapatite peaks is associated with the BC dissolution in contact with the acidic medium (Figure 1b). Manganese sorption with apatite phase can be, thus, anticipated either by the exchange with Ca through solid-state diffusion or a dissolution-precipitation mechanism. It was indicated that the dissolution reaction of biogenic hydroxyapatite is controlled by fast adsorption of protons on specific surface sites, followed by a slow removal of Mn by forming phosphate precipitate [$Mn_3(PO_4)_2 \cdot 7H_2O$] on the Apatite II^{TM} substrate [24]. Higher solubility of calcium fluorapatite compared to a manganese phosphate phase favored the dissolution-precipitation mechanism, in line with the evidenced mole-per-mole exchange between Mn and Ca in natural apatite [25]. Although the Mn-phosphate phase could not be identified in the BC residue due to the small concentration of Mn in the solid phase (9.62 mg/g) and the detection limits of the XRD technique, its formation cannot be dismissed.

Moreover, at the same BC dose, the Mn sorption increase decreases the final pH (Figure 3d). This phenomenon is characteristic of the specific cation sorption (chemisorption) that may also contribute to Mn removal by BC. The BC pH_{PZC} 6.9 (Table 2) signifies a solution pH value where the number of positively and negatively charged functional groups is balanced and a surface charge is neutral. The final pH values of interest for Mn sorption were lower than the pH_{PZC}, thus, BC exhibited an overall positive surface charge. In this case, the electrostatic attraction forces between the BC surface and the Mn(II) cannot contribute to the sorption [27]. Prevailing groups on hydroxyapatite surface in such conditions are positively charged $\equiv CaOH_2^+$ and neutral $\equiv POH^0$ species [21], and they may react with aqueous Mn through the surface complex formation:

$$\equiv CaOH_2^+ + Mn^{2+} <=> \equiv CaO\text{-}Mn^+ + 2H^+$$

$$2 \equiv CaOH_2^+ + Mn^{2+} <=> (\equiv CaO)_2Mn + 4H^+$$

$$\equiv POH + Mn^{2+} <=> \equiv POMn^+ + H^+$$

$$2 \equiv POH + Mn^{2+} <=> (\equiv PO)_2Mn + 2H^+$$

3.4. The Influence of Contact Time on Mn Removal

Based on the previous experiment, the manganese removal rate from the synthetic AMD (initial pH 2.5, 100 mg/L Mn) was investigated at 1.2 g/L WA and 10 g/L BC doses. Already after 5 min of contact, 70.3% of Mn was removed by BC and 20.7% by WA (Figure 4a,b). The efficiency of the treatment changed markedly up to 6 h, which was sufficient for the BC system to reach equilibrium (96%). The equilibrium time of Mn

removal from 100 mg/L solution at the initial pH of 5.8 was found to vary from several hours to a few days using a commercial bone char, depending on particle size and bone char/solution ratio [21]. On the other hand, WA removed 95.6% of Mn in 6 h, and the performance continued to increase up to 100% within 17 h of contact.
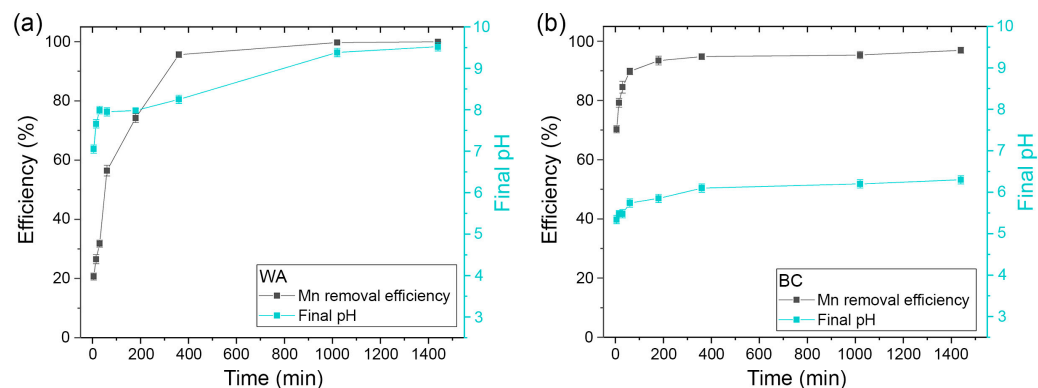

Figure 4. The effect of contact time on Mn removal by WA (**a**) and BC (**b**). Initial Mn concentration 100 mg/L, dose 1.2 g/L WA and 10 g/L BC, initial pH 2.5.

The amount of Mn removed per unit mass of reagents increased with time, reaching 83 mg/g of WA and 9.7 mg/g of BC at equilibrium conditions (Supplementary Material Figure S2d).

The final solution pH also increased with time (Figure 4a,b). WA required more time to achieve equilibrium pH (~17 h). The curve of pH change with time was complex, demonstrating the fast increase during the first 30 min, a quasi-plateau between 30 min and 3 h, and, subsequently, a slow increase until the equilibrium pH of 9.4. This trend results from heterogenous WA composition (Figure 1a) and different dissolution rates of mineral phases that contribute to the pH rise [46].

The Mn(II) is the prevalent state in natural waters [13]. The stability fields of manganese species in aqueous solution predicted by the Eh-pH diagrams depend on Mn activity, and for 100 mg/L Mn in solution, oxidation to Mn(III) and Mn(IV) and Mn_2O_3 and/or Mn_3O_4 precipitation in the absence of other species occur at pH $\geq$ 8 [47]. With WA, the final pH increased to the neutral range in the first minutes of contact (Figure 4a), in which the Mn(II) oxidation rate is very slow. Thus, initially, the uptake of Mn corresponds to Mn(II) removal by chemisorption at an overall positively charged WA surface (final pH < pH_{PZC}, Table 2). At pH > 8, particularly at pH 9, Mn(II) oxidation becomes faster and can be additionally accelerated if catalyzed by a solid surface or autocatalytic effect of the formed solid Mn oxide minerals [47]. Therefore, precipitation of Mn oxides occurred, as indicated by the complete disappearance of Mn from the solution.

The solution pH increased from 2.5 to 5.3 within 5 min reaction with BC. Fast carbonated hydroxyapatite dissolution in an acidic medium [24] increases pH and phosphate release significantly. In this period, as much as 70.3% of the Mn was removed, which strongly supports the dissolution and precipitation mechanism. Additionally, 26% Mn was removed with further pH increase from 5.3 to 6.2 up to 6 h of contact, and afterward, pH remained stable, as did Mn sorption.

3.5. The Influence of Sulfate Concentration

The concentration of sulfate anions in mine drainage effluents takes a wide range of values, typically from around five hundred to several thousand mg per liter [1]. Figure 5 shows variations in Mn removal efficiency with increased sulfate concentration for preselected conditions (initial pH 2.5, 100 mg/L Mn, doses of 1.2 g/L WA, and 10 g/L BC).
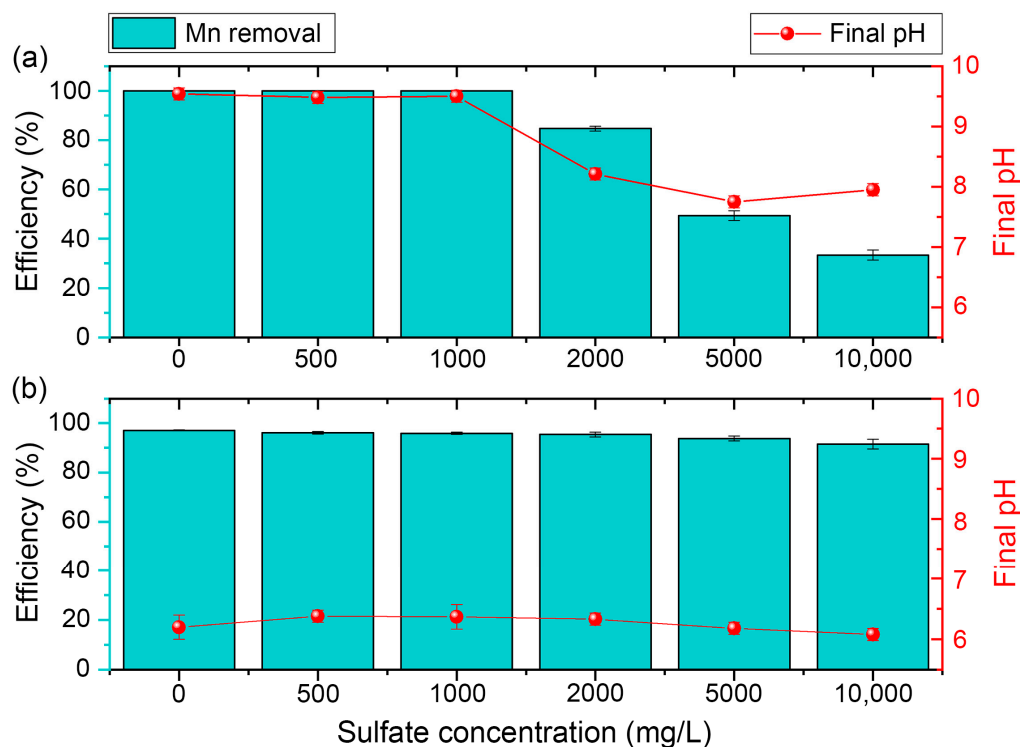
Figure 5. The effect of sulfate concentration on Mn removal by WA (**a**) and BC (**b**). Initial Mn concentration 100 mg/L, dose 1.2 g/L WA and 10 g/L BC, initial pH 2.5, contact time 24 h.

Up to 1000 mg/L, sulfate anions did not interfere with Mn removal. With WA, the final pH values of ~9.5 provided conditions for total Mn removal (Figure 5a). The presence of sulfate in the solution slows down the Mn oxidation rates even at pH > 9, at least in part due to the presence of the $MnSO_4$ (aq) complex [47]. However, the reaction time of 24 h was sufficient to accomplish complete Mn removal by oxidation/precipitation at such a pH. A decrease in WA efficiency to 84.7% occurred at 2000 mg/L sulfate and continued with increasing sulfate concentration so that at 10,000 mg/L, only 33.4% Mn was separated. In parallel, the solution pH gradually decreased, reaching a final pH of 8.0 at the highest sulfate concentration.

The variations in process efficacy and final pH values were considerably less pronounced when BC was added to synthetic AMD (Figure 5b). Over the entire range of sulfate concentration, the final pH was virtually constant (6.1 ± 0.1). Sulfate anions affected the process efficiency only at concentrations ≥ 2000 mg/L, causing the decrease to 91.5% at a concentration of 10,000 mg/L.

The amount of Mn removed per unit mass of reagents declined with the increase in sulfate content from 83.3 mg/g to 27.8 mg/g using WA and from 9.7 mg/g to 9.1 mg/g using the BC (Supplementary Material Figure S2e).

The residue of WA interaction with synthetic AMD having 10,000 mg/L sulfate shows high-intensity peaks of Ca_2SiO_4 and preserved MgO phase (Figure 1a). Also, the intensity of CaO peaks was reduced compared to pristine WA, the fairchildite ($K_2Ca(CO_3)_2$) dissolved completely, and the peaks of calcite appeared. The diffraction maximums of other newly formed phases are best matched with dipotassium silicate (Ks1: $K_2Si_4O_9$) and potassium aluminum sulfate hydrate (KaS: $KAl(SO_4)_2 \times 12H_2O$). The presence of extra low-intensity diffraction peaks in the XRD spectrum indicates the presence of other crystalline phases, which could not be identified reliably due to their low content and sample complexity. Precipitated sulfates may explain the limited solubility of primary pH regulating minerals, in line with the recorded final solution pH of 8.0, and the consequent adverse effect on Mn removal efficiency by WA.

On the other hand, the corresponding BC residue's crystal structure remained unchanged in relation to the starting BC (Figure 1b). Similarly, Fourier Transform Infrared (FTIR) spectra of the products from the natural fluorapatite reaction with Mn sulfate solution in the wide range of pH (2.0–7.0) did not differ from the FTIR spectrum of the starting material [25].

3.6. The Influence of Fe Concentration

Figure 6 displays the impact of coexisting Fe(II) ions on Mn removal by WA and BC and concurrent pH and Fe concentration changes. At a constant initial Mn concentration (100 mg/L) and preselected doses of reagents, an increase in Fe concentration negatively affected Mn ions removal efficiency. This effect was more pronounced with WA, causing a substantial decrease in Mn separation to 47.0% at Fe concentration of 100 mg/L and continuing steep fall, entirely blocking this process at 500 mg/L (Figure 6a). The removal of Fe ions from the solution was complete up to the highest initial Fe concentration of 500 mg/L, where a drop in Fe removal efficiency to 41.1% was also recorded.
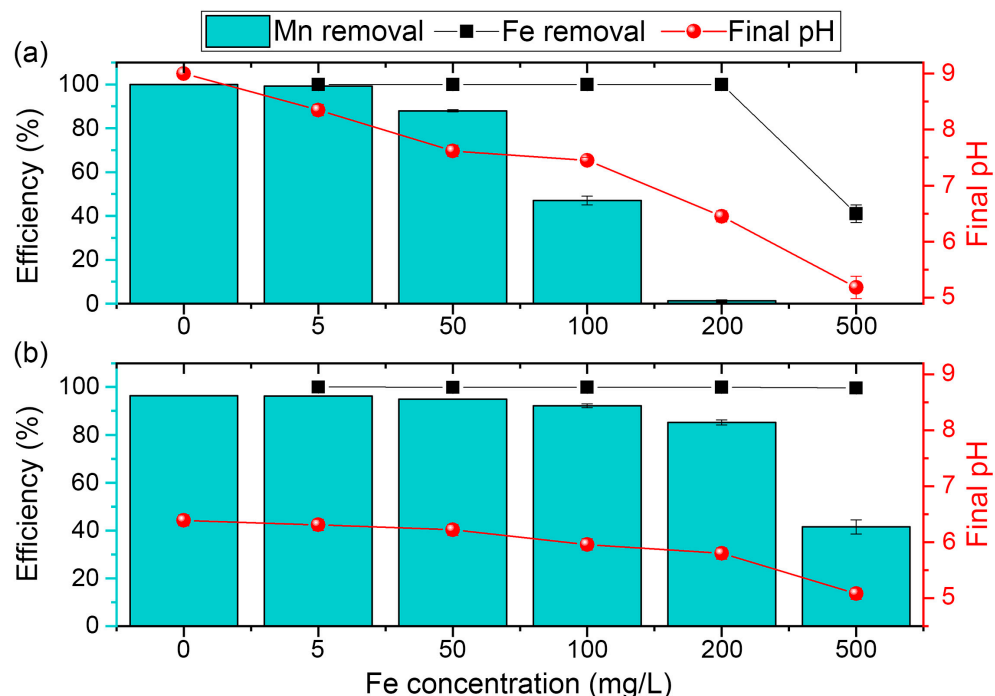

Figure 6. The effect of Fe concentration on Mn removal by WA (**a**) and BC (**b**). Initial Mn concentration 100 mg/L, dose 1.2 g/L WA and 10 g/L BC, initial pH 2.5, contact time 24 h.

These changes coincide with the significant pH decrease from 8.3 at 5 mg/L Fe to 5.2 at 500 mg/L Fe) (Figure 6a). The XRD spectra of the residue obtained at the concurrent Fe ions concentration of 500 mg/L demonstrate the exhaustion of the WA neutralization capacity (Figure 1a), with crystalline phases identified as periclase ($Mg_{0.99}Fe_{0.01}O$) and dipotassium hexacalcium pentadecaoxotetrasilicate (Kc: $K_2Ca_6Si_4O_{15}$).

Over the range of oxidation-reduction potentials characteristic for normal water environments, Fe (II) oxidizes to Fe (III), forming amorphous $Fe(OH)_3$ precipitates at pH > 5 [48]. Not only are lower pH and Eh conditions essential for the oxidation of Fe(II) compared to Mn(II), but the kinetics of the redox reactions of Fe(II) is also significantly faster [48]. Seeing the final pH values (Figure 6a), the co-removal of Mn and Fe by WA that took place in parallel up to their 1:2 ratio was governed by Fe oxidation and $Fe(OH)_3$ precipitation, whereas Mn was primarily removed by sorption. Sorption of Mn was likely enhanced by oxidation/precipitation at final pH > 8 (with 5 mg/L and 50 mg/L Fe) and declined rapidly

with the final pH decrease. When the Fe concentration reached 500 mg/L, even Fe removal was incomplete as the final pH was ~5.

The negative influence of Fe on Mn oxidation and precipitation at Fe/Mn ratios >4 was previously reported [13]. In the work of Calugaru et al. [49], half-calcined dolomite used at a dose of 7.5 g/L (0.3 g / 40 mL) was able to separate both metals efficiently at Mn concentrations up to ~100 mg/L and the Fe/Mn ratio of 10:1 as long as the equilibrium pH values were 9.7–9.8. However, keeping the same Fe/Mn ratio and increasing the initial Mn and Fe concentrations, a decrease in Fe and particularly Mn removal occurred due to a decrease in equilibrium pH to 6.8–6.9. The results of both our studies indicate the importance of the final pH in the system.

By applying BC, Mn removal of 96.2–85.2% was achieved from 5 mg/L Fe up to 200 mg/L Fe, while it declined to 41.5% at 500 mg/L Fe (Figure 6b). In parallel, Fe ions were entirely removed in all experimental runs, and the pH value of the solution decreased from 6.3 to 5.1 (Figure 6b). At initial pH 2.5, partial dissolution of a preselected dose of BC has provided a sufficient pH increase, phosphate anions release, and an abundance of active centers for effective Mn(II) removal by phosphate precipitation and chemisorption even at twice the concentration of Fe ions.

At initial Fe concentrations of 200 mg/L and 500 mg/L, the amount of Mn removed per unit mass of BC (8.5 mg/g and 4.1 mg/g) was higher compared to WA (1.0 mg/g and 0 mg/g) (Supplementary Material Figure S2f). Quantities of Fe removed by WA increased sharply from 4.2 to 167 mg/g with the increase in its concentration from 5 mg/L to 200 mg/L and reached a virtual plateau with further Fe concentration increase, whereas Fe amounts removed per gram of BC expanded from 0.5 mg/g to 49.9 mg/g, and the apparent linear trend indicates that the BC capacity was not exhausted (Supplementary Material Figure S3).

Apart from the characteristic carbonated hydroxyapatite peaks being of lower intensity, no other changes in the XRD spectrum of BC after interaction with 100 mg/L Mn and 500 mg/L Fe solution were detected (Figure 1b). In some previous investigations, Fe(II) sorption by apatite materials was anticipated. The study conducted with synthetic hydroxyapatite showed its high capacity (55.2 mg/g) for Fe, and it was attributed to Fe(II) ion exchange with Ca since the appearance of the Fe characteristic peaks in the EDS (Energy Dispersive Spectroscopy) spectrum of the residue coincided with a reduction in the intensity of the Ca peak [50]. Experiments with synthetic hydroxyapatite for the remediation of acidic mine drainage (initial pH 2.9) demonstrated more rapid Fe removal than Mn [51]. It was assigned to the sorption due to detected Ca release. However, the final pH values were not reported. Our study's final pH values of ≥ 5 imply possible Fe(II) oxidation/precipitation. On the other hand, at 500 mg/L Fe, BC removed Fe more efficiently than WA at the same final pH value of ~5, emphasizing that these two materials have different mechanisms of action. Additional experiments and analyses are necessary to address BC's mechanism of Fe removal.

3.7. Comparison of the Effects of Independent Process Variables

The selected responses (Mn and Fe removal efficiency, final pH) were monitored as a result of the simultaneous change in the levels of all input variables according to the matrix presented in Table 3. The combined influence of the process factors provoked Mn removal efficiency variation from 0% to 100%, and the applied design allowed the comparison of the effects of factors and identification of the most significant ones.

Table 3. Fractional factorial design matrix with a combination of factors levels in each experimental run and corresponding system responses.

Run	Independent Process Variables							Responses		
	Reagent	Mn (mg/L)	Sulfate (mg/L)	Fe (mg/L)	Time (h)	Initial pH	Dose (g/L)	Mn Removal(%)	Fe Removal (%)	Final pH
1	BC	100	10,000	5	0.5	2.0	5.0	26.6	93.4	4.9
2	WA	100	10,000	400	24	4.5	5.0	99.9	99.9	10.4
3	WA	5	1000	5	24	2.0	5.0	100	100	11.3
4	BC	5	1000	5	0.5	2.0	0.5	0	0	2.6
5	BC	100	1000	400	24	2.0	5.0	10.8	67.2	4.0
6	WA	5	1000	400	24	4.5	0.5	0	48.2	4.7
7	BC	100	10,000	400	0.5	4.5	0.5	2.4	2.9	4.8
8	BC	5	10,000	400	24	2.0	0.5	1.5	0	2.3
9	BC	5	10,000	5	24	4.5	5.0	99.4	100	6.9
10	WA	100	1000	5	0.5	4.5	5.0	99.9	100	11.6
11	WA	100	1000	400	0.5	2.0	0.5	0	1.2	2.4
12	WA	5	10,000	5	0.5	4.5	0.5	100	100	10.7
13	BC	5	1000	400	0.5	4.5	5.0	35.7	48.8	5.2
14	WA	100	10,000	5	24	2.0	0.5	0	0	2.4
15	WA	5	10,000	400	0.5	2.0	5.0	0	33.2	6.0
16	BC	100	1000	5	24	4.5	0.5	20.9	100	5.9

The main effects plot for Mn removal shows the calculated average response of each factor level and their distance from the overall average response for all variables presented by the horizontal line (Figure 7a). The critical impact on Mn removal can be ascribed to the variation of reagent dose, initial pH, and concentration of coexisting Fe ions. The changes in initial pH and solid/solution ratio from a lower to a higher level were beneficial for the process in contrast to increasing Fe concentration. A change of the reagent type from BC to WA displayed a slight positive effect on Mn removal, considering the average response of the system at all levels of all other factors. Finally, the effects of initial Mn and sulfate concentration and time were least pronounced.
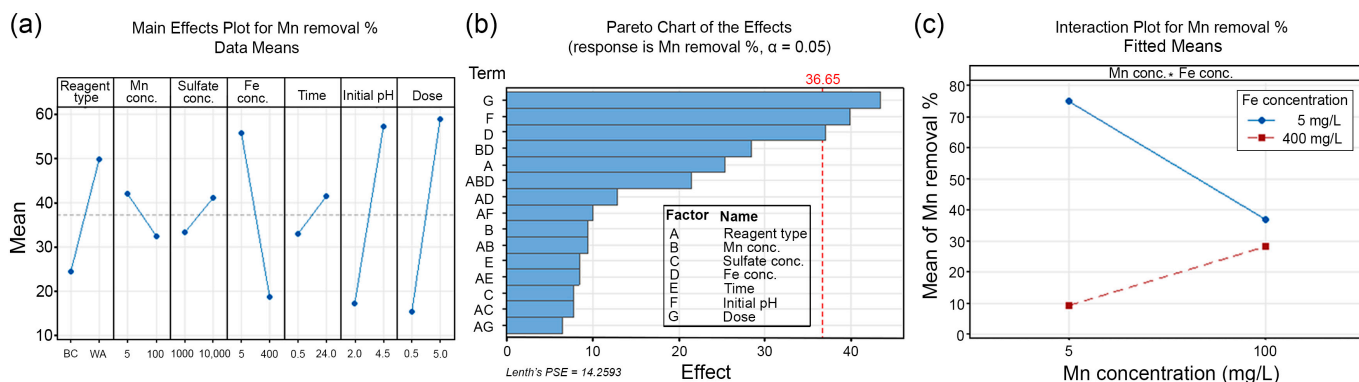

Figure 7. Main effect plots for Mn removal (**a**), Pareto chart of the effects of variables (**b**), and interaction plot for the effects of Mn and Fe concentrations (**c**).

The Pareto chart confirmed the significance (at $\alpha = 0.05$) of three main factors in the order: reagent dose > initial pH > Fe concentration (Figure 7b). None of the interaction effects (Supplementary Material Figure S4) displayed a statistical significance (Figure 7b), however, it is interesting to note that the effect of the Fe and Mn concentration (BD) interaction was most pronounced and higher compared to the main effects of the reagent type, Mn and sulfate concentration and contact time. As shown in Figure 7c, a higher Fe level hinders Mn removal by both reagents more significantly at lower than at higher Mn concentrations in the solution, confirming the importance of the Mn/Fe ratio.

Main effect plots for final pH and Fe removal efficiency as system responses (Supplementary Material Figure S5a,b) revealed common positive impacts of increasing reagent dose and initial pH and the negative impact of increasing initial Fe concentration. A change in the reagent type from BC to WA positively influenced the final pH. Nevertheless, none of the factors or their interactions were statistically significant at $\alpha = 0.05$ (Supplementary Material Figure S6a,b).

3.8. Relationship between Process Responses: Final pH and Mn Removal Efficiency

The change in the levels of individual factors and all factors simultaneously displayed the effect on Mn separation and final pH in WA and BC systems. To establish general relationships between these two system responses, the results (Figures 2–6, Table 3) are plotted as Mn removal efficiency against the final pH (Figure 8).
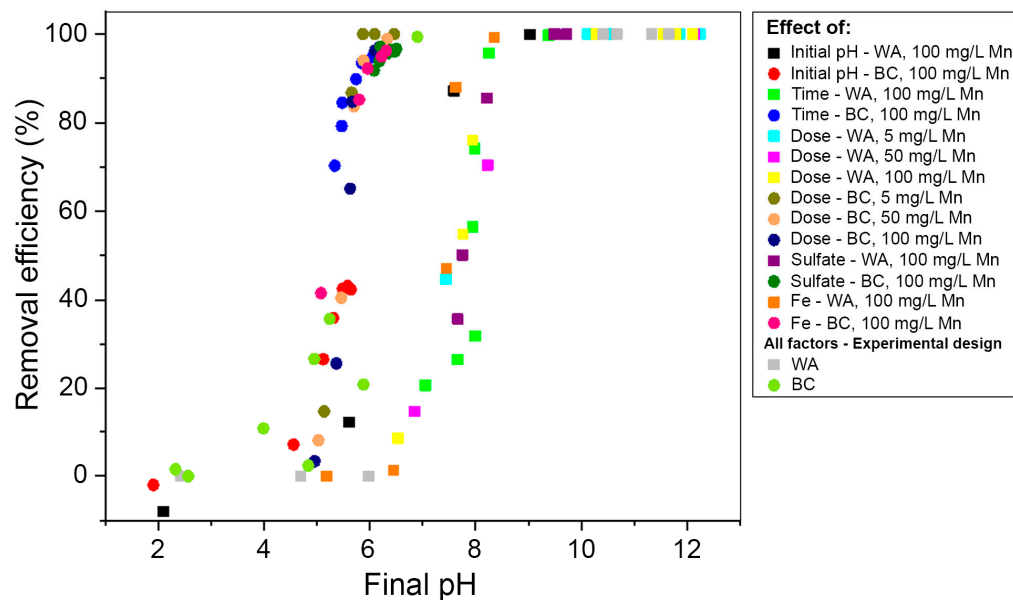

Figure 8. Relationships between the final pH and Mn removal efficiency by WA and BC under the influence of process factors.

Experimental data for different solid/solution ratios, initial pH, initial Mn, sulfate, Fe concentrations, and reaction times indicate a sharp Mn removal increase in narrow pH ranges, essentially separated according to the agents used. For BC, process efficiency was negligible below the final pH 5.0, while >95% for the final pH > 6.0. While previous studies outlined the importance of solution pH in Mn removal from AMD by apatite materials [22,25], the results from the present work link the influence of all examined factors on the process efficiency via the final pH values.

A pH of 8.4–9.0 was essential for Mn to precipitate as oxide and hydroxide during AMD treatment by various biomass ashes [38]. This study supports these findings and shows that Mn removal by WA shifts from insignificant at pH < 6.5 to complete at pH > 9.0 and takes place via Mn(II) sorption and oxidation/precipitation, depending on the pH in the system. The influence of high concentrations of coexisting species, insufficient time to dissolve alkaline WA minerals or a small dose of WA is reflected in less than 100% Mn removed because a critical final pH of 9 was not reached to make Mn(II) oxidation to higher oxidation states and deposition of Mn oxides thermodynamically favored.

3.9. Actual AMD Treatment with WA and BC

The actual AMD (Table 4) sample was characterized by a pH value of 3.4 and 116 mg/L of Mn. Additionally, AMD contained a high concentration of Zn (137 mg/L), significantly lower concentrations of Pb (1.92 mg/L), Ni (0.174 mg/L), Fe (0.140 mg/L), Cu (0.163 mg/L), Cd (0.264 mg/L), Co (0.072 mg/L), and Cr (0.008 mg/L).

Table 4. AMD composition before and after the treatment with WA and BC.

	AMD	WA Treatment 2.5 g/L	BC Treatment 30 g/L		AMD	WA Treatment 2.5 g/L	BC Treatment 30 g/L
pH	3.4 ± 0.1	9.0 ± 0.1	6.5 ± 0.1				
Element (mg/L)							
As	<0.005	<0.005	<0.005	Fe	0.140 ± 0.005	0.029 ± 0.001	0.015 ± 0.001
Al	2.89 ± 0.13	<0.005	<0.005	Mn	116 ± 4	0.061 ± 0.003	0.402 ± 0.020
Ba	<0.001	<0.001	<0.001	Ni	0.174 ± 0.09	<0.002	<0.002
Cd	0.264 ± 0.015	<0.001	<0.001	Pb	1.92 ± 0.10	<0.007	<0.007
Co	0.072 ± 0.003	<0.003	<0.003	Se	<0.002	<0.002	<0.002
Cr	0.008 ± 0.001	<0.001	<0.001	Zn	137 ± 9	0.013 ± 0.001	0.147 ± 0.008
Cu	0.163 ± 0.008	0.006 ± 0.001	0.024	V	<0.001	<0.001	<0.001

The variations in Mn removal efficiency and final pH values of AMD treated with WA and BC are presented in Figure 9. The increase in WA dose from 1.0 g/L to 3.0 g/L provoked a substantial pH rise from 7.0 to 9.4 and a consequential increase in Mn removal from 2.5% to 100%. At 2.5 g/L, 99.9% of Mn was removed at pH 9.0. Likewise, a rapid progression in Mn removal (4.2–90.1%) was detected as the quantity of applied BC raised from 1.0 g/L to 15 g/L. Process efficiency continued to increase with a further increase in the BC dose up to 30 g/L, gradually reaching 99.9%. In the entire range of BC doses, the final pH of AMD increased from 5.1 to 6.5.
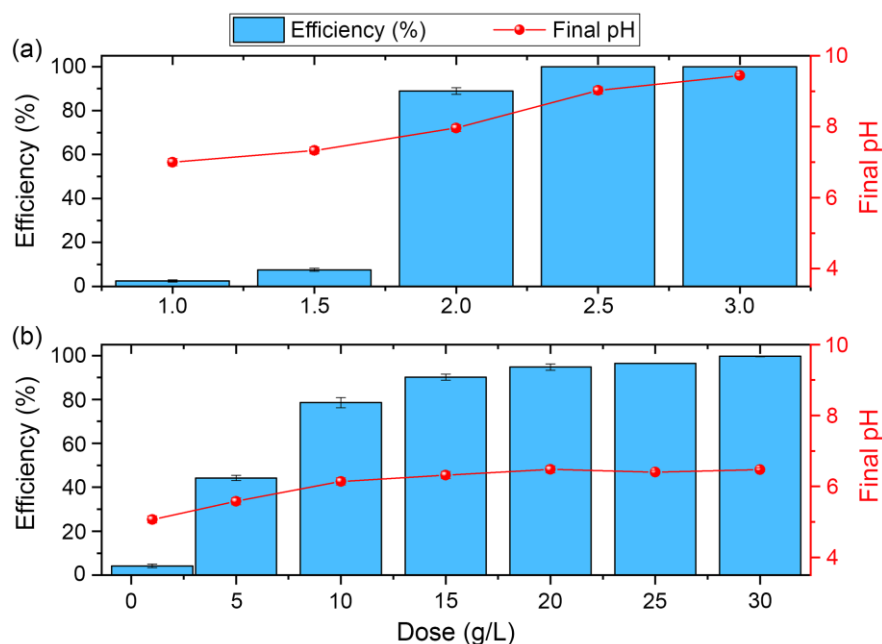
Figure 9. Mn removal efficiency and final pH values of actual AMD following the treatments by different doses of WA (**a**) and BC (**b**). Initial Mn concentration 116 mg/L, initial pH 3.4, contact time 24 h.

At AMD treatment conditions that can be considered optimal for Mn removal (2.5 g/L WA or 30 g/L BC), all coexisting metals were also effectively removed (Table 4). In agreement with the results obtained using synthetic AMD samples (Figure 8), this experiment confirms that successful removal of Mn from actual AMD is achievable by adjusting the doses of tested waste materials such as to provide a pH value of ≥9 after reaction with the WA, and a pH ~ 6.5, using the BC. However, the amount of BC to achieve this goal was twelve times the amount of WA, resulting in higher amounts of treatment residue.

WA and BC appear to be more practical agents for the remediation of Mn in AMD compared to limestone, which is a main precipitant due to its low cost and availability. By treatment of mine water at its natural pH (3.3) with 20.8 g/L of limestone, only 13% of the Mn initially present (16.5 mg/L) was removed, whereas the efficiency increased to 97%

when the initial pH of AMD was adjusted to 8.0 [52]. The application of limestone could not remove Mn effectively at high concentrations (140 mg/L), and even from synthetic solution with pH 6.5 and at high limestone doses (25 g/L), the Mn concentration was reduced to 120 mg/L [53]. However, 12.5 g/L of limestone mixed with 0.67 g/L sodium carbonate removed Mn completely from actual mine water with a pH of 6.5 as the final pH reached 9.6. For comparison, precipitation of 140 mg/L Mn with NaOH at pH 10 resulted in a residual metal concentration of 6.5 mg/L [53]. The actual AMD (pH 3.04; 5.94 mg/L Mn, 83.24 mg/L Fe) was also treated with waste biomaterials (shrimp shell (SS) and mussel byssus (MB)) [54]. The best removal efficiency of 96% for Fe and 78% for Mn was obtained with a mixture of waste materials (18 g/L SS and 10 g/L MB) when the final pH was 8.42 through the combined action of the sorption mechanisms on the biomaterials and precipitation as hydroxides. On the other hand, synthetic materials may show supremacy in Mn removal from AMD at much lower doses. For example, 0.5 g/L of hydroxyapatite (Hap) modified graphitic carbon nitride powders (Hap/gC_3N_4) applied in AMD with initial 3.5 and Mn concentration of 132.4 mg/L, removed 69% Mn [55].

3.10. The Stability of AMD Treatment Resides and Prospects for Metal Recovery

The stability of AMD treatment residues raises concerns about environmental and social impacts related to storage and disposal. Therefore, it was assessed by a batch test with deionized water. The concentrations of leachable elements measured in the liquid phase are expressed in mg/kg dry waste materials and compared with the threshold values set for the inert, nonhazardous, and hazardous wastes (Table 5).

Table 5. Water leachable concentrations of elements (mg/kg of dry waste material) in actual AMD treatment residues (EN 12457-2 test), and leaching limit values set by Council Decision 2003/33/EC for different waste categories.

	Actual AMD Treatment Residues		Waste Categories		
Element	WA	BC	Inert	Non-Hazardous	Hazardous
Al	173 ± 7	<LOD	-	-	-
As	<LOD	<LOD	0.5	2	25
Ba	0.518 ± 0.029	0.284 ± 0.012	20	100	300
Cd	<LOD	<LOD	0.04	1	5
Co	0.012 ± 0.005	0.023 ± 0.001	-	-	-
Cr	0.526 ± 0.022	0.005 ± 0.001	0.5	10	70
Cu	0.050 ± 0.002	0.050 ± 0.002	2	50	100
Fe	0.143 ± 0.006	0.129 ± 0.007	-	-	-
Mn	0.013 ± 0.002	5.940 ± 0.321	-	-	-
Mo	<LOD	<LOD	0.5	10	30
Ni	<LOD	<LOD	0.4	10	40
Pb	<LOD	<LOD	0.5	10	50
Sb	<LOD	<LOD	0.06	0.7	5
Se	<LOD	0.039 ± 0.002	0.1	0.5	7
V	<LOD	<LOD	-	-	-
Zn	0.488 ± 0.026	0.346 ± 0.018	4	50	200
pH	11.3 ± 0.1	7.1 ± 0.1	-	-	-

The concentrations of investigated elements were below the thresholds for inert waste, except for Cr in WA-residue (0.526 mg/kg vs. 0.5 mg/kg limit). Although not subject to classification, the leachable content of Al in WA-residue was substantial (173.3 mg/kg). The pH value of 11.3 was measured after resuspending this residue in deionized water, demonstrating high residual alkalinity. The enhanced leaching of Cr and Al over other metals can be attributed to the alkaline environment due to their amphoteric leaching behavior [56,57]. Given the neutral pH of the BC-residue (Table 5) and low concentrations of toxic and potentially toxic elements in pristine BC (Table 2), the leachability of all

tested elements was lower compared to WA, except for Mn (5.940 mg/kg), indicating higher stability.

The prospects for recovery of AMD major metals from the treatment residues are presented in Figure 10. With increasing HCl concentration, Mn and Zn release rates from WA residue significantly increased, from 0.7% to 127% and from 0% to 96%, respectively, as the final pH decreased from 8.5 to 0.34. In 1 mol/L HCl, WA residue was virtually completely dissolved, thus releasing the Mn from the AMD treatment process and the WA composition (Table 2). Considering the BC residue (Figure 10b), Mn recovery with 0.01 mol/L HCl at final pH 5.3 was 7.2%, while Zn detachment was marginal (0.13% and 0.68%). The Mn and Zn recovery reached maximally 93% and 95% in 1 mol/L HCl due to almost complete BC residue dissolution at the final pH of 0.2.
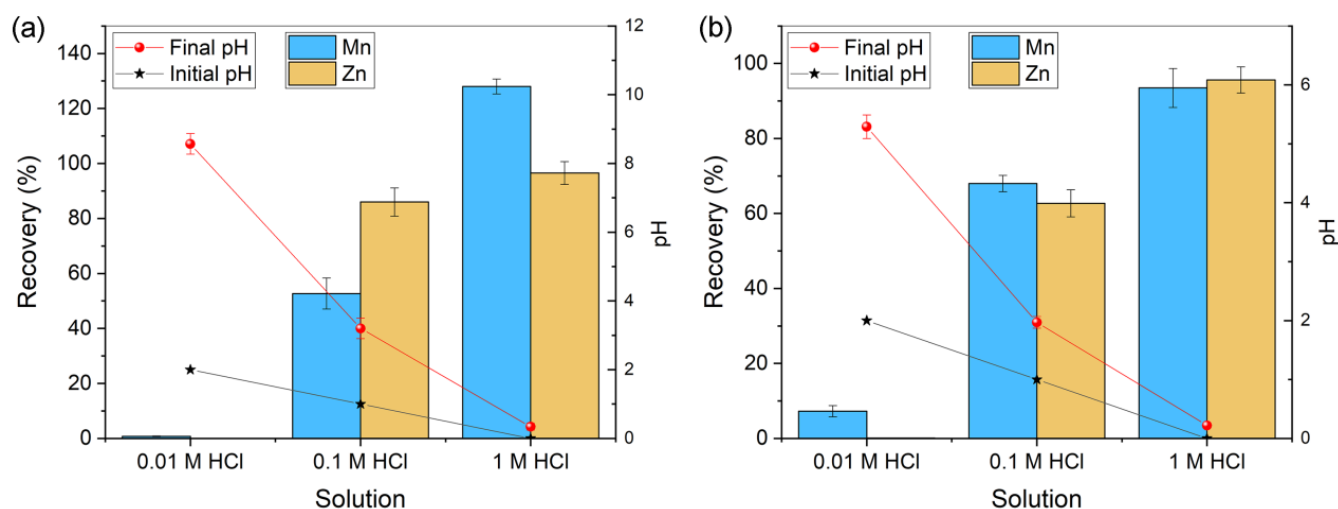
Figure 10. Recovery of AMD major cations (Mn and Zn) from WA (**a**) and BC (**b**) treatment residues using 0.1 mol/L $CaCl_2$, 0.01 mol/L HCl, 0.1 mol/L HCl, and 1 mol/L HCl. Solid to solution ratio 5 g/L, contact time 24 h.

Since the pH levels profoundly influence the removal of Mn, it is plausible to anticipate that the release of Mn ions could be facilitated by controlling the pH in the system. Notably, mineral acids, particularly HCl, exhibited remarkable efficacy in regenerating materials such as adsorptive membranes [58] and nanocarbon hybrid [59], which had previously sequestered Mn from solution via ion exchange or physical adsorption. The successful reuse of the sorbent underscores the preservation of its physical and chemical properties over several sorption-desorption cycles. However, results depicted in Figure 10 confirm that precipitated and chemisorbed forms of Mn were released when the residues were subjected to high acid concentrations, resulting in the dissolution of the materials employed. While recyclability is paramount for costly synthetic and modified materials [60], the regeneration of WA and BC, as waste and waste-derived materials, would present a modest economic rationale. Consequently, utilizing these residues in alternative technologies and for metal recovery emerges as a more pragmatic option.

4. Conclusions

Insight into the performance of unconventional reagents concerning AMD properties and other process factors can accelerate their practical application. This study's results show that wood ash and bone char can be valuable materials for Mn treatment in AMD and emphasize their use's comparative advantages and disadvantages. The summary key points and recommendations are following:

- Complete separation of Mn in AMD occurs only at final pH > 9.0 using WA. The WA is a cost-effective alternative to conventional alkaline reagents such as lime, and its consumption is attractive from environmental protection and circular economy

standpoints. However, the issue of the high alkalinity of the treated water and the generated residue remains.

- The BC application is advantageous compared to WA for its ability to separate Mn at close to neutral conditions and faster establishment of equilibrium conditions. Furthermore, BC is a more useful reagent for treating sulfate-rich AMD, showing a 5% decrease in Mn removal efficiency up to sulfate concentrations of 10,000 mg/L. The influence of coexisting Fe ions up to a Fe/Mn ratio of 5:1 is significantly lower using BC.
- The impact of all investigated process factors and their interactions on Mn removal efficiency can be seen indirectly through their ability to bring the pH to or further from the optimal pH values for BC or WA action. Such insight helps optimize the conditions of the Mn removal process by adjusting the pH value in the system, which can be done successfully by optimizing the reagent dose.
- Depending on the AMD pH and composition, 3–12 times smaller quantities of WA than BC are needed, generating less residue. Still, the alkalinity of the WA-treatment residue impacts the enhanced leaching of elements with amphoteric leaching behavior, posing a potential risk to the environment.
- Further studies on potential hazards due to metal release from the residues should consider the conditions of their disposal or reuse. The reuse options for the residues of AMD treatment with WA and BC are particularly interesting, for instance, in metals recovery, prevention and control of AMD, or stabilization of contaminated soil. Given the high BC/AMD ratio needed to effectively treat high Mn concentrations at low pH, previous pH adjustment to a near-neutral region using a low-cost alkalizer would significantly reduce the required BC dose. In that sense, applying wood ash and BC in two consecutive steps is worth exploring.

References

1. Hill, R.D. *Mine Drainage Treatment: State of the Art and Research Needs*; U.S. Department of the Interior, Mine Drainage Control Activities, Federal Water Pollution Control Administration: Cincinnati, OH, USA, 1968.
2. Park, I.; Tabelin, C.B.; Jeon, S.; Li, X.; Seno, K.; Ito, M.; Hiroyoshi, N. A review of recent strategies for acid mine drainage prevention and mine tailings recycling. *Chemosphere* **2019**, *219*, 588–606. [CrossRef] [PubMed]
3. Skousen, J.G.; Ziemkiewicz, P.F.; McDonald, L.M. Acid mine drainage formation, control and treatment: Approaches and strategies. *Extr. Ind. Soc.* **2019**, *6*, 241–249. [CrossRef]
4. Kefeni, K.K.; Msagati, T.A.M.; Mamba, B.B. Acid mine drainage: Prevention, treatment options, and resource recovery: A review. *J. Clean. Prod.* **2017**, *151*, 475–493. [CrossRef]
5. Skousen, J. Overview of acid mine drainage treatment with chemicals. In *Acid Mine Drainage, Rock Drainage, and Acid Sulfate Soils*; John Wiley & Sons, Inc.: Hoboken, NJ, USA, 2014; pp. 325–337.
6. Jiao, Y.; Zhang, C.; Su, P.; Tang, Y.; Huang, Z.; Ma, T. A review of acid mine drainage: Formation mechanism, treatment technology, typical engineering cases and resource utilization. *Process Saf. Environ. Prot.* **2023**, *170*, 1240–1260. [CrossRef]
7. Johnson, D.B.; Hallberg, K.B. Acid mine drainage remediation options: A review. *Sci. Total Environ.* **2005**, *338*, 3–14. [CrossRef] [PubMed]
8. European Commission. *A New Circular Economy Action Plan For a Cleaner and More Competitive Europe*; COM(2020) 98 Final. Communication from the Commission to the European Parliament, the Council, the European Economic and Social Committee and the Committee of the Regions; EC: Brussels, Belgium, 2020; pp. 1–19.
9. Li, Y.; Li, W.; Xiao, Q.; Song, S.; Liu, Y.; Naidu, R. Acid mine drainage remediation strategies: A review on migration and source controls. *Miner. Metall. Process.* **2018**, *35*, 148–158. [CrossRef]
10. Lucas, H.; Stopic, S.; Xakalashe, B.; Ndlovu, S.; Friedrich, B. Synergism red mud-acid mine drainage as a sustainable solution for neutralizing and immobilizing hazardous elements. *Metals* **2021**, *11*, 620. [CrossRef]
11. Westholm, L.J.; Repo, E.; Sillanpää, M. Filter materials for metal removal from mine drainage—A review. *Environ. Sci. Pollut. Res.* **2014**, *21*, 9109–9128. [CrossRef]
12. Howe, P.D.; Malcolm, H.M.; Dobson, S. *; World Health Organization & International Programme on Chemical Safety. Manganese and Its Compounds: Environmental Aspects*; World Health Organization: Geneva, Switzerland, 2004; pp. 1–63.
13. Neculita, C.M.; Rosa, E. A review of the implications and challenges of manganese removal from mine drainage. *Chemosphere* **2019**, *214*, 491–510. [CrossRef]
14. Matveeva, V.A.; Alekseenko, A.V.; Karthe, D.; Puzanov, A.V. Manganese pollution in mining-influenced rivers and lakes: Current state and forecast under climate change in the Russian Arctic. *Water* **2022**, *14*, 1091. [CrossRef]
15. Li, Y.; Xu, Z.; Ma, H.; Hursthouse, S.A. Removal of manganese(II) from acid mine wastewater: A review of the challenges and opportunities with special emphasis on Mn-oxidizing bacteria and microalgae. *Water* **2019**, *11*, 2493. [CrossRef]
16. Rudi, N.N.; Muhamad, M.S.; Te Chuan, L.; Alipal, J.; Omar, S.; Hamidon, N.; Abdul Hamid, N.H.; Mohamed Sunar, N.; Ali, R.; Harun, H. Evolution of adsorption process for manganese removal in water via agricultural waste adsorbents. *Heliyon* **2020**, *6*, e05049. [CrossRef] [PubMed]
17. Chowdhury, S.; Mishra, M.; Suganya, O. The incorporation of wood waste ash as a partial cement replacement material for making structural grade concrete: An overview. *Ain Shams Eng. J.* **2015**, *6*, 429–437. [CrossRef]
18. Heviánková, S.; Bestová, I.; Kyncl, M. The application of wood ash as a reagent in acid mine drainage treatment. *Miner. Eng.* **2014**, *56*, 109–111. [CrossRef]
19. Fawell, J.; Bailey, K.; Chilton, J.; Dahi, E.; Fewtrell, L.; Magara, Y. *Fluoride in Drinking-Water*, 1st ed.; World Health Organization: Geneva, Switzerland, 2006; pp. 1–134.
20. Kono, T.; Sakae, T.; Nakada, H.; Kaneda, T.; Okada, H. Confusion between carbonate apatite and biological apatite (carbonated hydroxyapatite) in bone and teeth. *Minerals* **2022**, *12*, 170. [CrossRef]
21. Sicupira, D.C.; Silva, T.T.; Leão, V.A.; Mansur, M.B. Batch removal of manganese from acid mine drainage using bone char. *Brazilian J. Chem. Eng.* **2014**, *31*, 195–204. [CrossRef]
22. Sicupira, D.C.; Tolentino Silva, T.; Ladeira, A.C.Q.; Mansur, M.B. Adsorption of manganese from acid mine drainage effluents using bone char: Continuous fixed bed column and batch desorption studies. *Brazilian J. Chem. Eng.* **2015**, *32*, 577–584. [CrossRef]
23. Carrillo-González, R.; González-Chávez, M.C.A.; Cazares, G.O.; Luna, J.L. Trace element adsorption from acid mine drainage and mine residues on nanometric hydroxyapatite. *Environ. Monit. Assess.* **2022**, *194*, 280. [CrossRef]
24. Oliva, J.; Cama, J.; Cortina, J.L.; Ayora, C.; De Pablo, J. Biogenic hydroxyapatite (Apatite II^{TM}) dissolution kinetics and metal removal from acid mine drainage. *J. Hazard. Mater.* **2012**, *213–214*, 7–18. [CrossRef]
25. Vandeginste, V.; Cowan, C.; Gomes, R.L.; Hassan, T.; Titman, J. Natural fluorapatite dissolution kinetics and Mn^{2+} and Cr^{3+} metal removal from sulfate fluids at 35 °C. *J. Hazard. Mater.* **2020**, *389*, 122150. [CrossRef]
26. Nayak, A.; Bhushan, B. Hydroxyapatite as an advanced adsorbent for removal of heavy metal ions from water: Focus on its applications and limitations. *Mater. Today Proc.* **2021**, *46*, 11029–11034. [CrossRef]
27. Brazdis, R.I.; Fierascu, I.; Avramescu, S.M.; Fierascu, R.C. Recent progress in the application of hydroxyapatite for the adsorption of heavy metals from water matrices. *Materials* **2021**, *14*, 6898. [CrossRef]
28. Amenaghawon, A.N.; Anyalewechi, C.L.; Darmokoesoemo, H.; Kusuma, H.S. Hydroxyapatite-based adsorbents: Applications in sequestering heavy metals and dyes. *J. Environ. Manag.* **2022**, *302*, 113989. [CrossRef]

29. Dimović, S.; Smičiklas, I.; Plećaš, I.; Antonović, D.; Mitrić, M. Comparative study of differently treated animal bones for Co^{2+} removal. *J. Hazard. Mater.* **2009**, *164*, 279–287. [CrossRef]

30. Smičiklas, I.; Dimović, S.; Šljivić, M.; Plećaš, I.; Lončar, B.; Mitrić, M. Resource recovery of animal bones: Study on sorptive properties and mechanism for Sr^{2+} ions. *J. Nucl. Mater.* **2010**, *400*, 15–24. [CrossRef]

31. Fiol, N.; Villaescusa, I. Determination of sorbent point zero charge: Usefulness in sorption studies. *Environ. Chem. Lett.* **2009**, *7*, 79–84. [CrossRef]

32. *PDXL: Integrated X-ray Powder Diffraction Software*, Version 2.0.3.0; Rigaku Corporation: Tokyo, Japan, 2011; 196–8666.

33. Gates-Rector, S.; Blanton, T. The powder diffraction file: A quality materials characterization database. *Powder Diffr.* **2019**, *34*, 352–360. [CrossRef]

34. Downs, R.T.; Hall-Wallace, M. The American mineralogist crystal structure database. *Am. Mineral.* **2003**, *88*, 247–250.

35. *BS EN 12457-2*; Characterisation of Waste. Leaching. Compliance Test for Leaching of Granular Waste Materials and Sludges. Part 2: One Stage Batch Test at a Liquid to Solid Ratio of 10 L/kg for Materials with Particle Size below 4 mm (without or with Size Reduction). British Standards Institue: London, UK, 2002.

36. Vassilev, S.V.; Baxter, D.; Andersen, L.K.; Vassileva, C.G. An overview of the chemical composition of biomass. *Fuel* **2010**, *89*, 913–933. [CrossRef]

37. Campbell, A.G. Recycling and disposing of wood ash. *Tappi J.* **1990**, *73*, 141–146.

38. Bogush, A.A.; Dabu, C.; Tikhova, V.D.; Kim, J.K.; Campos, L.C. Biomass ashes for acid mine drainage remediation. *Waste Biomass Valor.* **2020**, *11*, 4977–4989. [CrossRef]

39. Garvie, L.A.J. Mineralogy of paloverde (*Parkinsonia microphylla*) tree ash from the Sonoran Desert: A combined field and laboratory study. *Am. Mineral.* **2016**, *101*, 1584–1595. [CrossRef]

40. Von Euw, S.; Wang, Y.; Laurent, G.; Drouet, C.; Babonneau, F.; Nassif, N.; Azaïs, T. Bone mineral: New insights into its chemical composition. *Sci. Rep.* **2019**, *9*, 8456. [CrossRef] [PubMed]

41. Barbu, C.H.; Pavel, P.B.; Moise, C.M.; Sand, C.; Pop, M.R. Neutralization of acid mine drainage with wood ash. *Rev. Chim.* **2018**, *68*, 2768–2770. [CrossRef]

42. Labaali, Z.; Kholtei, S.; Naja, J. Co^{2+} removal from wastewater using apatite prepared through phosphate waste rocks valorization: Equilibrium, kinetics and thermodynamics studies. *Sci. Afr.* **2020**, *8*, e00350. [CrossRef]

43. Bin Mobarak, M.; Pinky, N.S.; Chowdhury, F.; Hossain, M.S.; Mahmud, M.; Quddus, M.S.; Jahan, S.A.; Ahmed, S. Environmental remediation by hydroxyapatite: Solid state synthesis utilizing waste chicken eggshell and adsorption experiment with Congo red dye. *J. Saudi Chem. Soc.* **2023**, *27*, 101690. [CrossRef]

44. Ganta, D.D.; Hirpaye, B.Y.; Raghavanpillai, S.K.; Menber, S.Y. Green synthesis of hydroxyapatite nanoparticles using *Monoon longifolium* leaf extract for removal of fluoride from aqueous solution. *J. Chem.* **2022**, *2022*, 4917604. [CrossRef]

45. Kalembkiewicz, J.; Galas, D.; Sitarz-Palczak, E. The physicochemical properties and composition of biomass ash and evaluating directions of its applications. *Polish J. Environ. Stud.* **2018**, *27*, 2593–2603. [CrossRef]

46. Petronijević, N.; Radovanović, D.; Štulović, M.; Sokić, M.; Jovanović, G.; Kamberović, Ž.; Stanković, S.; Stopic, S.; Onjia, A. Analysis of the mechanism of acid mine drainage neutralization using fly ash as an alternative material: A case study of the extremely acidic Lake Robule in eastern Serbia. *Water* **2022**, *14*, 3244. [CrossRef]

47. Hem, J.D. *Chemical Equilibria and Rates of Manganese Oxidation*; Water Supply Paper 1667-A; U.S. G.P.O.: Washington, DC, USA, 1963; pp. A1–A64. [CrossRef]

48. Liu, J.; Chen, Q.; Yang, Y.; Wei, H.; Laipan, M.; Zhu, R.; He, H.; Hochella, M.F. Coupled redox cycling of Fe and Mn in the environment: The complex interplay of solution species with Fe- and Mn-(oxyhydr)oxide crystallization and transformation. *Earth-Science Rev.* **2022**, *232*, 104105. [CrossRef]

49. Calugaru, I.L.; Genty, T.; Neculita, C.M. Treatment of manganese, in the presence or absence of iron, in acid and neutral mine drainage using raw vs half-calcined dolomite. *Miner. Eng.* **2021**, *160*, 106666. [CrossRef]

50. Brundavanam, S.; Poinern, G.E.J.; Fawcett, D. Kinetic and adsorption behaviour of aqueous Fe^{2+}, Cu^{2+} and Zn^{2}+ using a 30 nm hydroxyapatite based powder synthesized via a combined ultrasound and microwave based technique. *Am. J. Mater. Sci.* **2015**, *5*, 31–40.

51. Popa, M.; Bostan, R.; Varvara, S.; Moldovan, M.; Rosu, C. Removal of Fe, Zn and Mn ions from acidic mine drainage using hydroxyapatite. *J. Environ. Prot. Ecol.* **2016**, *17*, 1472–1480.

52. Silva, A.M.; Cruz, F.L.S.; Lima, R.M.F.; Teixeira, M.C.; Leão, V.A. Manganese and limestone interactions during mine water treatment. *J. Hazard. Mater.* **2010**, *181*, 514–520. [CrossRef] [PubMed]

53. Silva, A.M.; Cunha, E.C.; Silva, F.D.R.; Leão, V.A. Treatment of high-manganese mine water with limestone and sodium carbonate. *J. Clean. Prod.* **2012**, *29–30*, 11–19. [CrossRef]

54. Núñez-Gómez, D.; Lapolli, F.R.; Nagel-Hassemer, M.E.; Lobo-Recio, M.Á. Optimization of Fe and Mn removal from coal acid mine drainage (AMD) with waste biomaterials: Statistical modeling and kinetic study. *Waste Biomass Valor.* **2020**, *11*, 1143–1157. [CrossRef]

55. Agha Beygli, R.; Mohaghegh, N.; Rahimi, E. Metal ion adsorption from wastewater by g-C_3N_4 modified with hydroxyapatite: A case study from Sarcheshmeh acid mine drainage. *Res. Chem. Intermed.* **2019**, *45*, 2255–2268. [CrossRef]

56. Cui, Y.; Chen, J.; Zhang, Y.; Peng, D.; Huang, T.; Sun, C. pH-dependent leaching characteristics of major and toxic elements from red mud. *Int. J. Environ. Res. Public Health* **2019**, *16*, 2046. [CrossRef]

57. Smičiklas, I.; Jović, M.; Janković, M.; Smiljanić, S.; Onjia, A. Environmental safety aspects of solid residues resulting from acid mine drainage neutralization with fresh and aged red mud. *Water Air Soil Pollut.* **2021**, *232*, 490. [CrossRef]
58. Vo, T.S.; Hossain, M.M.; Jeong, H.M.; Kim, K. Heavy metal removal applications using adsorptive membranes. *Nano Converg.* **2020**, *7*, 36. [CrossRef]
59. Embaby, M.A.; Abdel Moniem, S.M.; Fathy, N.A.; El-kady, A.A. Nanocarbon hybrid for simultaneous removal of arsenic, iron and manganese ions from aqueous solutions. *Heliyon* **2021**, *7*, e08218. [CrossRef] [PubMed]
60. Mokgehle, T.M.; Tavengwa, N.T. Recent developments in materials used for the removal of metal ions from acid mine drainage. *Appl. Water Sci.* **2021**, *11*, 42. [CrossRef]